Molecular and Cellular Pathobiology

Cancer Research

Interaction between *MYC* and *MCL1* in the Genesis and Outcome of Non–Small-Cell Lung Cancer

Thaddeus D. Allen[1], Chang Qi Zhu[2], Kirk D. Jones[3], Naoki Yanagawa[2], Ming-Sound Tsao[2,4], and J. Michael Bishop[1]

Abstract

MYC exerts both positive and negative functions in cancer cells, such that its procancerous effects are unmasked only after its anticancer effects are blocked. Here we used multiple mouse models of lung adenocarcinoma to identify genetic events that can cooperate with MYC activation to promote the genesis of non–small-cell lung cancer (NSCLC), the most common form of lung cancer in humans. MYC overexpression targeted to pulmonary alveolar cells was sufficient to induce lung adenomas and carcinomas. Tumorigenesis was assisted by either spontaneous mutations in *Kras* or experimental introduction of activated RAS, but investigations revealed that additional events were required to circumvent apoptosis, one of the most significant negative functions exerted by MYC. We determined that overexpression of the antiapoptotic protein MCL1 was sufficient to circumvent apoptosis in this setting. Previous clinical studies have indicated that prognosis of human NSCLC is not associated with MCL1, despite its overexpression in many NSCLCs. In reexamining the prognostic value in this setting, we found that MCL1 overexpression does correlate with poor patient survival, but only when accompanied by MYC overexpression. Our findings therefore produce a convergence of mouse and human results that explain how MCL1 can block an important negative consequence of MYC overexpression in both experimental models and clinical cases of NSCLC. *Cancer Res; 71(6); 2212–21. ©2011 AACR.*

Introduction

Overexpression of the protooncogene *MYC* has been implicated in the genesis of multiple human malignancies (1). *MYC* encodes a transcription factor that regulates gene networks controlling proliferation, metabolism, and ribosome biogenesis (2–4). However, *MYC* overexpression also activates the proapoptotic BCL2 family protein BAX (5, 6) leading to the release of cytochrome *c* and apoptosis (7). Compensatory genetic and/or epigenetic alterations are required to diminish the antitumorigenic effects of *MYC* and tip the balance in favor of malignant growth (8, 9).

Here we have used mouse models to uncover events that enable the genesis of lung tumors initiated by *MYC*. Targeting expression of *MYC* to pulmonary alveolar cells gave rise to adenomas and carcinomas. Tumorigenesis was assisted by spontaneous mutations in *Kras*, but also required an additional event to circumvent apoptosis. One such event proved to be overexpression of the antiapoptotic protein MCL1.

MCL1 is an antiapoptotic member of the BCL2 family of proteins that localizes to the outer mitochondrial membrane, as well as other intracellular membranes (10). It inhibits apoptosis by interfering with mitochondrial events that lead to cytochrome *c* release (11, 12). *MCL1* is amplified in human NSCLC (13) and cooperates with *MYC* in experimental leukemogenesis (14, 15).

Previous work has suggested that MCL1 overexpression does not correlate with prognosis in NSCLC (16, 17). We reexamined the prognostic value of MCL1 expression in NSCLC and found that MCL1 overexpression does correlate with poor patient survival, but only when accompanied by overexpression of the MYC protein. We suggest that the joint overexpression of MCL1 and MYC may be a useful biomarker for both prognosis and treatment in human NSCLC. In particular, inhibition of MCL1 might have a synthetic lethal effect by unleashing the proapoptotic effect of MYC.

Methods

Transgenic mice

Protocols were carried out with approval of the Institutional Animal Care and Use Committee (IACUC) of the University of California, San Francisco. Transgenic mice expressing the reverse tetracycline transactivator (rtTA; ref. 18) and mice carrying a human *MYC* transgene under the transcriptional

Authors' Affiliations: [1]G.W. Hooper Research Foundation, University of California, San Francisco; [2]Ontario Cancer Institute/Princess Margaret Hospital, Toronto, Ontario, Canada; [3]Department of Pathology and Laboratory Medicine, University of California, San Francisco; and [4]Department of Laboratory Medicine and Pathobiology, Department of Medical Biophysics, University of Toronto, Canada

Note: Supplementary data for this article are available at Cancer Research Online (http://cancerres.aacrjournals.org/).

Corresponding Author: Thaddeus D. Allen, University of California, San Francisco, 513 Parnassus Avenue, HSW 1501, San Francisco, CA. Phone: 415-476-5350; Fax: 415-476-6185. E-mail: Thaddeus.Allen@ucsf.edu

doi: 10.1158/0008-5472.CAN-10-3590

control of a tetracycline-response element (TRE) promoter (19) have been previously described. Lung phenotypes were evaluated according to criteria recommended by the Mouse Models of Human Cancer Consortium (20).

Taqman analysis

RNA was extracted using the Absolutely RNA Miniprep kit (Stratagene). Total RNA was reverse-transcribed using Stratascript reverse transcriptase (Stratagene), and cDNA was analyzed by realtime-PCR (Taqman, Applied Biosystems). Relative gene expression was normalized to a mouse β-*Actin* Taqman probe.

Mouse tissue staining

Immunohistochemical staining was carried out using the Vector Elite ABC Kit (Vector Laboratories) and TUNEL staining was done using the ApopTag Peroxidase *In Situ* Apoptosis Detection Kit (Chemicon). For BrdU labeling, mice were injected with 100 mg/kg BrdU (BD Pharmingen) 2 hours prior to sacrifice. $BrdU^+$ cells were detected using anti-BrdU mouse monoclonal B44 (BD Biosciences).

Protein analysis

Western blot analysis was carried out using standard protocols. Information regarding the antibodies utilized is available upon request. RAS activity was measured in 250 μg of whole lung or tumor protein lysate using a RAS Activation Assay Kit (Millipore).

Sequencing

The entire coding sequences for *Kras*, *Nras*, and *Hras* were cloned into the vector pCR2.1 using a TA Cloning kit (Invitrogen). A mutation was deemed present when 2 or more clones harbored the same nucleic acid change in comparison to the wild-type allele. We sequenced 10 clones per sample.

MNU treatments

Mice were injected once intraperitoneally at 4 weeks of age with 50 mg/kg *N*-methyl-*N*-nitrosourea (MNU) and monitored for up to 6 months post injection. Tumors present on the pleural surface were enumerated using a dissecting scope.

***In vivo* transduction of alveolar hyperplasia**

Transgenic mice were treated with DOX 24 hours prior to tracheal injection of retrovirus. Anesthetized mice were intubated and concentrated viral particles were directly introduced to the airways via the intubation tube using a syringe and needle. Afterwards, cohorts of transduced mice were either kept free of doxycycline (DOX) or fed a DOX diet to continuously induce *MYC*. Ecotropic retrovirus was produced using standard techniques. The pMig retroviral plasmid (21) was utilized as it encoded the enhanced green fluorescent protein (EGFP) downstream of an internal ribosomal entry site (IRES). A final volume of 100 μL of viral suspension ($>1\times10^6$ retroviral particles) was used per injection.

Immunohistochemistry of the NSCLC tissue microarray

Immunohistochemistry (IHC) was carried out following procedures previously described (22). The primary antibodies were rabbit polyclonals raised against either the human MYC (N-262) or MCL1 protein (S-19), both from Santa Cruz Biotechnology. Details regarding tissue microarray (TMA) construction, scoring and statistical analysis are found in Supplementary Methods.

Results

Activation of *MYC* induces alveolar hyperplasia and apoptosis

We created mouse models in which *MYC* expression could be induced with DOX with the aim of examining the earliest stage of *MYC*-induced lung tumorigenesis. Transgenic mice expressing rtTA under the control of either the human surfactant protein C (SPC) promoter (S transgene) or the rat Clara cell secretory protein (CCSP) promoter (C transgene) were used to achieve lung specific expression (Fig. 1A; ref. 18). Endogenous SPC is expressed in alveolar type II pneumocytes and CCSP in Clara cells of the upper airway. However, the fidelity of the CCSP expression pattern is not maintained by the C transgene (18). Both the S and C transgenes are transcriptionally active mainly in type II cells and the main distinction between the 2 transgenes appears to be the level of DOX-inducible expression that can be achieved. We bred S and C mice to mice carrying a human *MYC* transgene under the transcriptional control of a TRE promoter (TM transgene) (19). A diet supplemented with DOX was used to stimulate the transactivating function of the rtTA protein and induce *MYC* in the resulting SPC-rtTA/TRE-*MYC* (STM) and CCSP-rtTA/TRE-*MYC* (CTM) mice.

Transgenic lungs were examined for *MYC* mRNA expression after 2, 4, and 7 days of DOX. As expected, expression of *MYC* was not detected in S mice (data not shown). TM and CTM mice had detectable levels of transcription from the *MYC* transgene (Fig. 1B and data not shown) but MYC protein remained below the level of detection by Western blot analysis (Fig. 1C). In contrast, we observed a substantial but transient rise in *MYC* transgene mRNA in STM mice, with a concomitant increase in MYC protein. This coincided with the appearance of alveolar hyperplasia, which was abundant in STM mice (Fig. 1E) but absent from CTM mice (data not shown) where *MYC* expression was lower. Alveolar hyperplasia formed as clusters of cells that expanded the alveolar septa, reached a maximum after 4 days of DOX treatment and then resolved (Fig. 1F). We pulse-labeled proliferating cells using BrdU. Clusters of $BrdU^+$ cells were common in the alveolar space after 4 days of DOX treatment (Fig. 1H), but not after 7 days (Fig. 1I). We also detected $TUNEL^+$ cells (Fig. 1K). As alveolar hyperplasia resolved, TUNEL staining declined to near background levels (Fig. 1L). We concluded that in the alveolar epithelium MYC-induced proliferation was restrained by MYC-induced apoptosis. Eradication of cells by this apoptosis could explain the transience of detectable MYC expression in response to DOX.

Mice that overexpress *MYC* develop lung adenomas and adenocarcinomas

Reduced lifespan was observed for STM and CTM mice, both treated with DOX after weaning and in the absence of

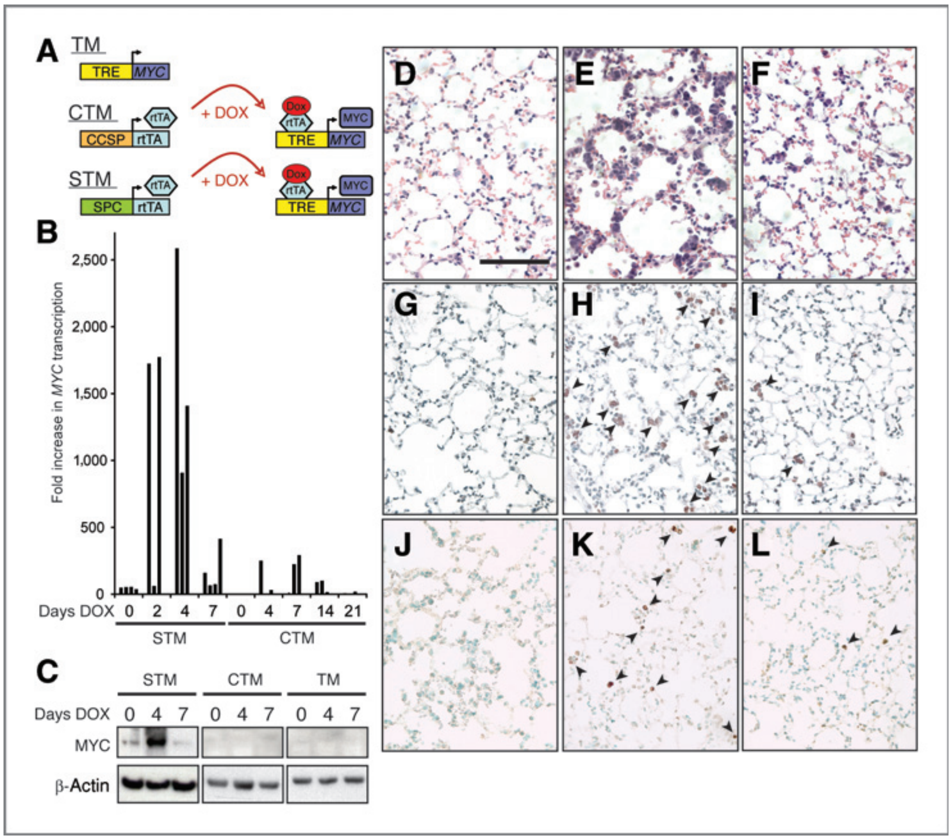

Figure 1. Overexpression of *MYC* induced alveolar hyperplasia and apoptosis. A, schematic of transgenes used for *MYC* overexpression (see descriptions in text). B, analysis of transgenic *MYC* expression using whole lung RNA and a human-specific Taqman probe. Each bar represents an individual mouse (n = 3–4 each time-point; error bars not seen since deviation in individual mouse replicates was insubstantial). Values were normalized to the average background level of transcription detected in mice carrying the TM transgene alone (n = 6 mice). C, Western blot analysis of MYC levels in whole lung protein extracts. D–F, H&E staining; G–I, BrdU staining; and J–L, TUNEL staining of lungs of STM mice exposed to DOX for 0 (D, G, J), 4 (E, H, K), and 7 (F, I, L) days (bar in D equals 0.1 mm; D–L, same magnification).

DOX, but not in a cohort of DOX-treated TM mice (Fig. 2A). STM and CTM mice treated with DOX did fare worse than untreated mice, but decreases in survival did not reach statistical significance (Log-rank; $P = 0.108$ for STM and $P = 0.052$ for CTM mice).

After 18 months only solid adenomas were found in 73.3% ($n = 15$) of the DOX-treated TM mice (Fig. 2B, C, D). In contrast, STM and CTM mice developed both papillary adenomas and adenocarcinomas (Fig. 2B, E-G) with DOX increasing the penetrance of adenocarcinoma from 31.6% ($n = 19$) to 57.9% ($n = 19$) and 23.8% ($n = 21$) to 56.7% ($n = 30$) in STM and CTM mice respectively (Fig. 2B). Tumorigenesis was rarely multifocal and respiratory distress was observed only when an adenocarcinoma expanded to occlude an entire lobe of the lung (Fig. 2H) or the upper respiratory tract (Fig. 2I). Metastases (Fig. 2J) were observed only in DOX-treated STM (1 of 17, 5.9%) and CTM (5 of 30, 16.7%) mice.

Our findings suggest that even MYC expression below the limit of detection by Western blot analysis can predispose to lung tumorigenesis. Despite the initial low levels of MYC, the resulting adenomas and adenocarcinomas both had higher levels of MYC protein than normal lung samples (100% of tumors; Fig. 3A), and tumors from DOX-treated mice always had very high levels of MYC. Given the ability of MYC to elicit apoptosis in pulmonary epithelium, we reasoned that an antiapoptotic function must emerge during the course of tumorigenesis elicited by activation of the *MYC* transgene. We sought to define events that occurred in lung tumors to allow bypass of MYC-induced apoptosis.

Tumors induced by *MYC* overexpression harbor activating *Kras* mutations

We immunostained lung tumors from STM and CTM mice for proteins expressed in lung epithelial lineages. Tumors from both genotypes resembled tumors elicited by mutant RAS (23–25) in being TTF-1$^+$, SPC$^+$, and CCSP$^-$ (Supplementary Fig. 1). This suggested that the pathogenesis of tumors in STM and CTM mice might also involve activated RAS. We assayed RAS activity and found elevated activity in all the *MYC* transgenic tumors (Supplementary Fig. 2). Sequencing of *Ras* genes revealed activating *Kras* mutations in 100% of the tumors (Fig. 3B). As adenomas harbored *Kras* mutation (4/4 adenomas; 7/7 adenocarcinomas; 0/4 control lungs), we presume that the mutations occurred before the transition from adenoma to adenocarcinoma. We concluded that mutant RAS and MYC cooperated in lung tumorigenesis in our *MYC* transgenic mice.

Overexpression of *MYC* impedes tumorigenesis by activated RAS

It is widely held that RAS blocks MYC-induced apoptosis through the PI3K/AKT pathway, whereas RAS-induced senescence is overcome by MYC-induced proliferation (26). Therefore, we reasoned that signaling downstream of activated

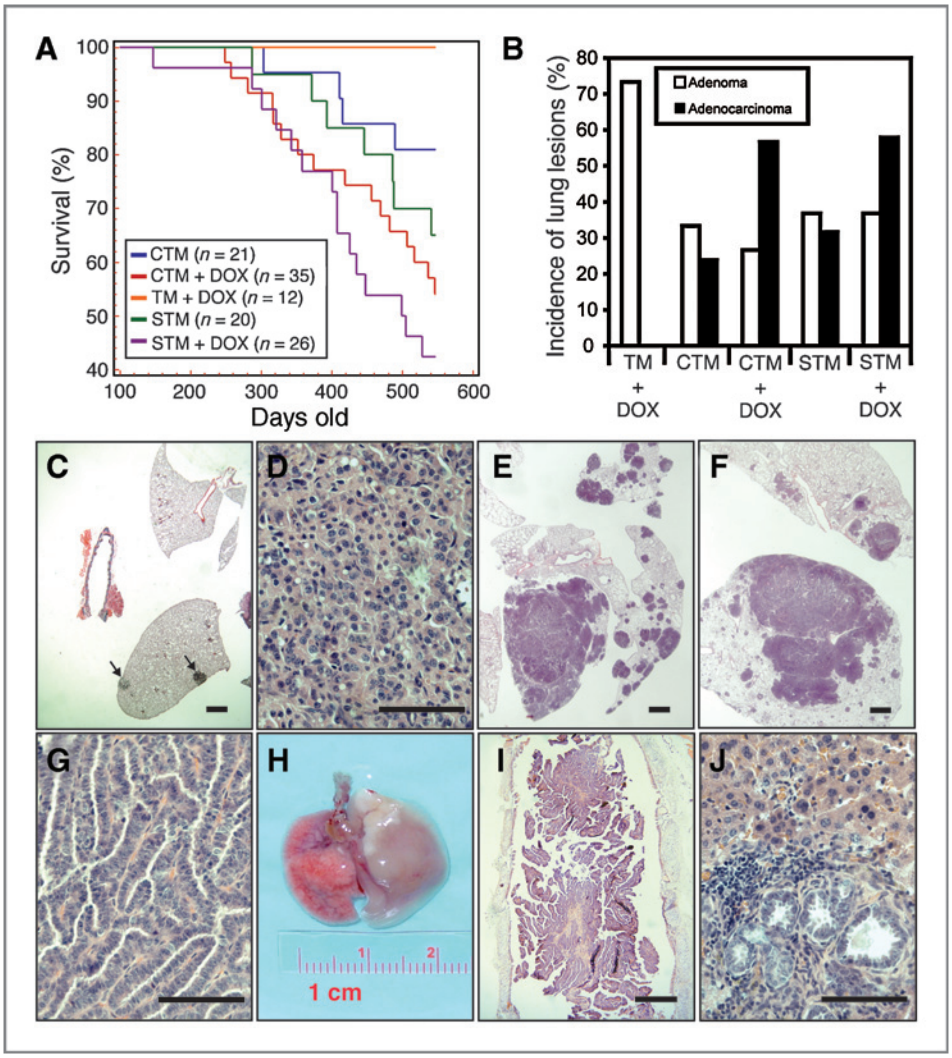

Figure 2. Mice overexpressing *MYC* developed lung adenomas and adenocarcinomas.A, Kaplan–Meier plot. B, graphical representation of lung tumor incidence in transgenic mice. The cumulative numbers of tumors up until 18 months is displayed. C-G & I-J, H&E stained sections from *MYC* transgenic mice. Adenomas (C, arrows) in TM mice remained small with well-circumscribed borders and a solid growth pattern (D). Large adenocarcinomas surrounded by smaller foci, presumably due to intra-pulmonary spread from the main tumor mass, could often be observed in DOX-fed STM (E) and CTM (F) mice. G, papillary patterning of an adenocarcinoma from a DOX-fed STM mouse. H, lung and trachea whole-mount. In this DOX-fed STM mouse, tumor tissue grew to occlude the entire left lobe of the lung before the mouse became moribund. I, adenocarcinoma invading the trachea of a CTM mouse. J, liver metastases with acinar histology from an STM mouse (bar in C, E, F, and I equals 1 mm; bar in D, G and J equals 0.1 mm).

KRAS might be responsible for abrogation of MYC-induced apoptosis in lung tumorigenesis.

In an initial effort to explore this possibility, we treated mice with the DNA-alkylating agent *N*-methyl-*N*-nitrosourea (MNU) to jump-start tumorigenesis with a synchronous wave of mutagenesis in *Kras* (27). As expected, all the lung tumors from MNU-treated mice harbored activating *Kras* mutation (data not shown). The survival of TM mice was unaffected by MNU (Fig. 4A; data not shown for DOX-free mice), as these mice only developed a few adenomas (Fig. 4B; data not shown). In contrast, treatment of STM mice with MNU substantially accelerated their usual rate of demise (Fig. 4A; compare with Fig. 2A) as adenocarcinomas developed in both the DOX-treated and untreated groups. STM mice fed a DOX diet fared better than untreated mice (Fig. 4A; Log-rank, $P < 0.02$) and had a significantly lower number of tumors compared with mutagenized STM mice kept on a DOX-free diet (Fig. 4B; *t* test, $P < 0.002$). Therefore, *MYC* induction hindered, rather than aided MNU-induced tumorigenesis. These results present an apparent paradox when compared with those in Figure 2, where activation of the *MYC* transgene exacerbated tumorigenesis. We attribute the paradox to the different time frames of tumorigenesis in the 2 sets of experiments. The relatively rapid course of tumorigenesis in response to MNU might reduce the likelihood that an antiapoptotic event could occur in time to protect developing tumor cells from the proapoptotic effect of MYC.

We further explored the interaction between MYC and activated RAS through retroviral transduction of alveolar hyperplasia (Fig. 4C). In brief, we gave STM mice DOX for 1 day prior to tracheal instillation of concentrated retrovirus encoding mutant RAS. DOX induced the *MYC* transgene and the proliferation of alveolar cells, a prerequisite for retroviral infection of the otherwise quiescent alveolar epithelium. Transduction was not successful in DOX-treated CTM mice (data not shown), in which the level of *MYC* induction was below the threshold required to induce hyperplasia (see aforementioned).

Our initial proof-of-concept experiments utilized retrovirus expressing activated human *HRAS* and *EGFP* downstream of

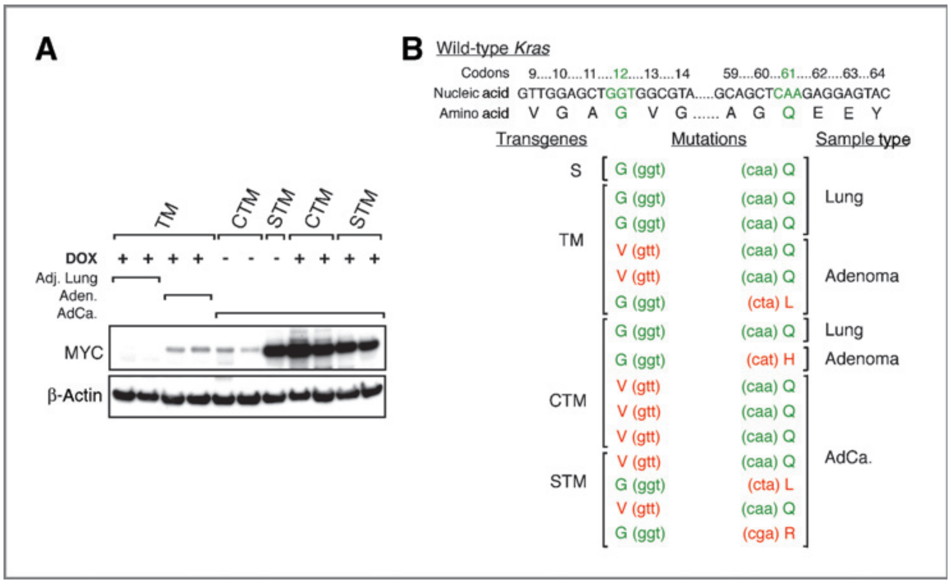

Figure 3. *MYC* transgenic tumors have activating mutations in *Kras*. A, Western blot analysis of MYC expression in normal lung, adenomas, and adenocarcinomas from transgenic mice. B, spectrum of mutations detected in *Kras* from tumors from DOX-fed *MYC* transgenic mice (Green = wild-type, Red = mutant).

an internal ribosomal entry site so that cells expressing activated RAS would be marked. We found that activated forms of both *Kras* and *HRAS* induced identical tumor phenotypes in this assay. As with NMU-treated animals, transduction with activated RAS accelerated the demise of STM mice (Fig. 4D). Continuous DOX administration increased survival (Log-rank, $P < 0.002$) and 2 of 5 mice remained tumor-free (Supplementary Fig. 3A). In contrast, mice treated with DOX only for the 24 hours prior to transduction developed multiple adenomas and adenocarcinomas (Fig. 4E, F), and adenomas could be detected as early as 1 month following transduction (Fig. 4G). Only solitary transduced cells were found in mice treated with DOX for one month ($n = 4$ mice) (Fig. 4H). At least some of these cells maintained their tumorigenic potential, however, because removal of DOX after one month resulted in tumors (Supplementary Fig. 3B) and intermediate survival (Fig. 4D). The data present the same paradox in comparison with Figure 2 as observed with MNU. We presume that the same explanation applies.

Our results suggest that the antitumor effects of *MYC* are not mitigated by activated RAS. This proved to be the case both in the MNU mutagenesis experiment, where activated *Kras* was expressed from its endogenous promoter, and when activated RAS was ectopically expressed using retrovirus.

MCL1 overexpression allows the progression of *MYC* overexpressing tumors

We reasoned that *MYC* transgenic tumors must harbor additional tumorigenic changes and took a candidate gene approach to search for antiapoptotic events that could account for the ability of transgenic tumors to overexpress MYC. Caspases, members of the inhibitor of apoptosis protein (IAP) family and members of the BCL2 protein family were measured by Western blotting of lysate from tumors and adjacent normal tissue (data not shown and see legend to Fig. 5). This approach yielded 1 candidate, MCL1, an antiapoptotic member of the BCL2 family of proteins (28). MCL1 was overexpressed in one STM and one CTM adenocarcinoma (2/13 in total; Fig. 5A and data not shown). This suggested that MCL1 overexpression could be an adaptive trait acquired by some tumors to offset MYC-induced apoptosis. Other, unknown antiapoptotic events presumably fulfilled a similar role in transgenic tumors not overexpressing MCL1.

To validate that MCL1 cooperated with MYC, we utilized retroviral transduction to introduce *Mcl1* or *Kras*^{G12V} alone, or both *Kras*^{G12V} and *Mcl1* together into STM mice (Fig. 5B). Retrovirus expressing only *Mcl1* had no tumorigenic effect in STM mice ($n = 8$, data not shown). Like mice transduced with *HRAS*^{G12V} retrovirus (Fig. 4E, F), both *Kras*^{G12V} and *Kras*^{G12V}/*Mcl1* transduced mice had a high tumor burden when placed on a DOX-free diet (Supplementary Fig. 4A, B). There was no significant difference in their survival (Supplementary Fig. 4C). In contrast, continuous induction of the *MYC* transgene (Supplementary Fig. 4D) reduced the tumor burden in *Kras*^{G12V} transduced mice (Fig. 5D) but not in *Kras*^{G12V}/*Mcl1* transduced mice (Fig. 5E), and the former had significantly better survival relative to the latter (Fig. 5C; log-rank, $P < 0.05$).

Kras^{G12V}/*Mcl1* tumors from DOX-fed STM mice had a mixed morphology of papillary adenocarcinoma interspersed with areas of large cell undifferentiated carcinoma (Fig. 5F) that lacked the expression of differentiation markers (Supplementary Fig. 5). This contrasts with the strictly papillary growth in the tumors of the original CTM and STM mice (see Fig. 2G). In human NSCLC, lack of differentiation is correlated with poor prognosis (29). It appears that the *Kras*^{G12V}/*Mcl1* tumors from mice given DOX to induce *MYC* may mimic aggressive human NSCLCs.

Presumably, the effects of MCL1 stemmed from its ability to protect against MYC-induced apoptosis, as MCL1 overexpression did not alter either expression of MYC (Supplementary Fig. 4D) or RAS activity (Supplementary Fig. 4E). We concluded

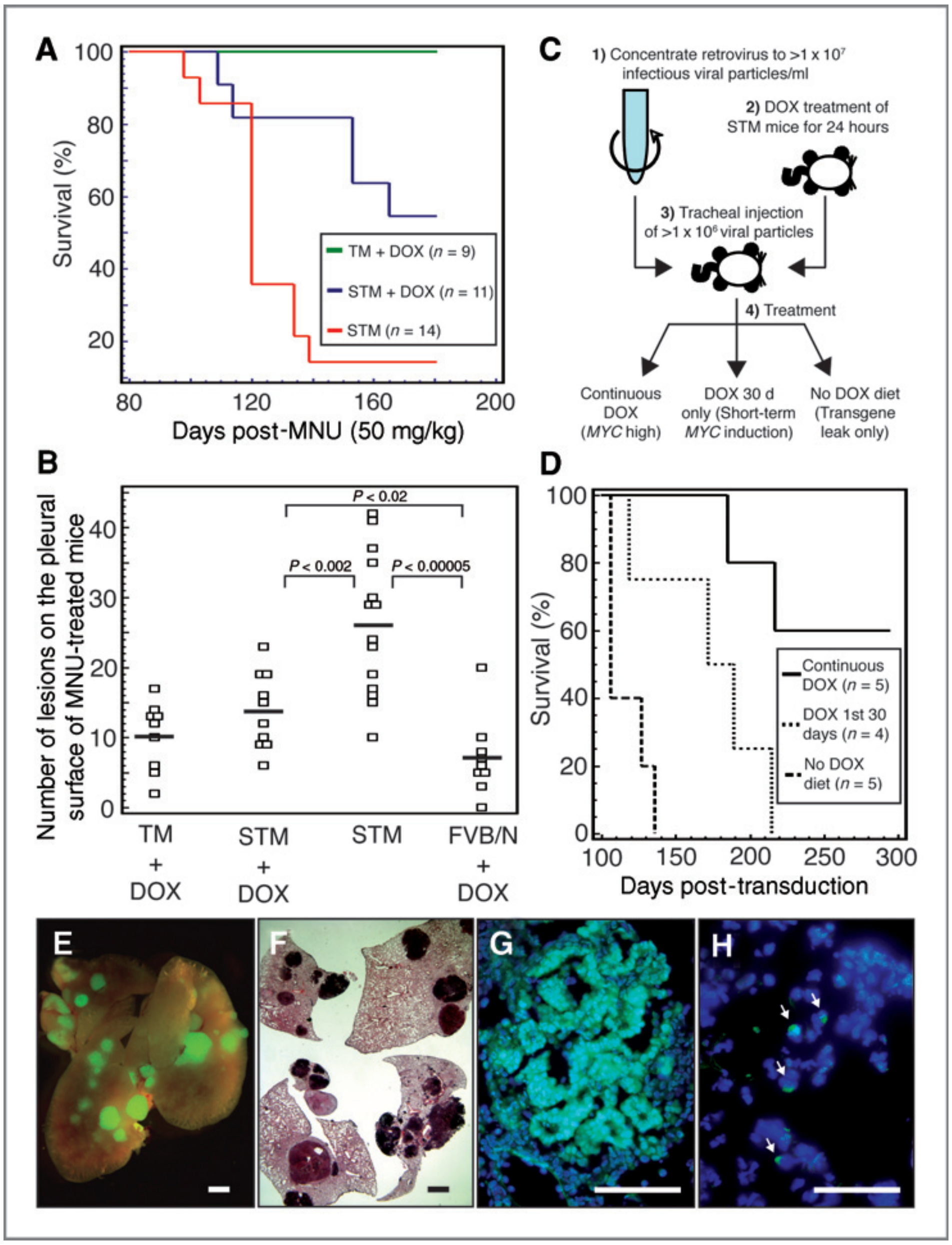

Figure 4. Activation of the *MYC* transgene inhibits tumorigenesis induced by activated RAS. A, Kaplan–Meier plot. Mice were administered 50 mg/kg MNU intraperitoneally and monitored for up to 6 months. B, lesions visible on the pleural surface were quantified to compare tumor burden in MNU treated mice. Statistical significance was assessed using the Student's *t* test. C, schematic diagram outlining the protocol used to retrovirally transduce hyperplastic alveolar cells in STM mice. D, Kaplan–Meier plot of mice transduced with pMig-*HRAS*^{G12V}. DOX treatment varied after transduction as indicated. E, EGFP expression from an internal ribosomal entry site found in the pMig retroviral vector allowed tracking of transduced cells. Multiple EGFP$^+$ adenomas and adenocarcinomas could be found 4 to 6 months after pMig-*HRAS*^{G12V} infection when mice were fed a DOX-free diet. F, H&E-stained lung section of a pMig-*HRAS*^{G12V}-infected mouse after 4 months on a DOX-free diet. G, frozen section showing an EGFP$^+$ adenoma from a pMig-*HRAS*^{G12V}-infected mouse fed a regular diet for 1 month after transduction (blue DAPI counter-stain). H, 1 month of DOX treatment was not sufficient to completely eliminate pMig-*HRAS*^{G12V}-transduced cells. EGFP$^+$ cells could still be found in the alveolar region after one month of DOX treatment (arrows; bar in E and F equals 1 mm; bar in G and H equals 0.1 mm).

that MCL1 acted as an oncogene, but its tumorigenic potential was manifest only when MYC was overexpressed.

Combined high MCL1 and MYC expression is a poor prognostic indicator in NSCLC

To explore whether the interaction between MCL1 and MYC has biological significance in human NSCLC, we evaluated their expression by IHC. Compared with normal lung tissue, MYC and MCL1 were each overexpressed in a subset of tumors (Supplementary Table 1, Supplementary Fig. 6). High expression of MYC and MCL1 was detected in 30.5% and 49.1% of the tumors, respectively. Of the MYC overexpressing tumors, 72.2% also overexpressed MCL1 (Table 1, Fig. 6A). Therefore, MYC and MCL1 overexpression overlapped significantly (22% of all the NSCLCs examined).

A trend was observed for both MYC (Table 1) and MCL1 (Supplementary Table 2) to be highly expressed in NSCLCs that were less differentiated, a finding that prompted us to examine the correlation of combined expression with prognosis. Among the 59 NSCLCs with full follow-up (demographics in Table 1), neither MYC nor MCL1 expression alone was prognostic (data not shown). However, 2 completely different outcomes were observed when tumors expressing MCL1 were stratified by MYC expression. Whereas high expression of MCL1 was marginally associated with better survival when MYC was not

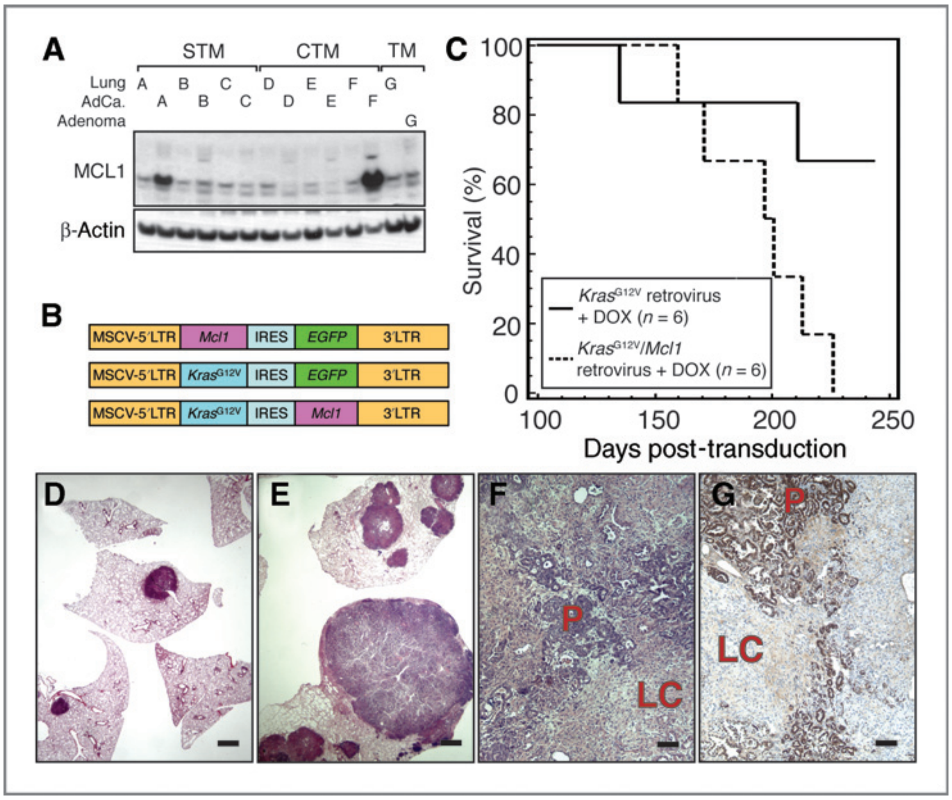

Figure 5. MCL1 acts as an oncoprotein when coexpressed with MYC. A, of the antiapoptotic BCL2 family proteins screened by Western blot analysis of lysates from lungs and tumors of DOX-treated *MYC* transgenic mice (BCL2, BCL2L1/BCL-X_L, BCL2L2/BCLW, BCL2A1/BFL1, MCL1), only MCL1 was elevated in a subset of adenocarcinomas. Letters denote individual mice. B, retroviral constructs used to introduce *Mcl1*, $Kras^{G12V}$ or both $Kras^{G12V}$ and *Mcl1* together into hyperplastic alveolar cells of STM mice. C, Kaplan–Meier plot comparing the survival of mice fed a DOX diet following transduction with retrovirus encoding $Kras^{G12V}$ alone or both $Kras^{G12V}$ and *Mcl1* together (Log-rank, $P < 0.05$). D–F, H&E-stained sections. D, lungs of an STM mouse transduced with $Kras^{G12V}$-expressing retrovirus and continuously fed a DOX diet to induce *MYC* overexpression. E, lungs of an STM mouse transduced with retrovirus coexpressing $Kras^{G12V}$ and *Mcl1* together and fed a DOX diet. F, a tumor from a DOX-fed $Kras^{G12V}$/*Mcl1* mouse showing large areas of both papillary adenocarcinoma (marked P) and large cell undifferentiated carcinoma (marked LC) in the same tumor mass. G, immunohistochemical staining for TTF-1 clearly demarcates the transition zone between papillary (TTF-1^+) and large cell (TTF-1^-) histology (bar in D and E equals 1 mm; bar in F and G equal 0.1 mm).

expressed ($P = 0.0738$; Fig. 6B), it was significantly associated with poorer overall survival when MYC was expressed ($P = 0.0142$, Fig. 6C). The data suggest that high MCL1 and MYC expression may cooperate during the genesis of a subset of human NSCLCs and combined expression has implications for patient survival. A likely explanation for our findings is that MCL1 facilitates NSCLC progression by impeding MYC's proapoptotic function.

Discussion

The origin of tumors in *MYC* transgenic mice

MYC induction in STM mice led to the formation of alveolar hyperplasia. However, apoptosis soon cleared hyerplastic cells. Pleomorphic, proliferative cells have previously been noted in mice constitutively expressing *MYC* under control of the SPC promoter (30). These cells also succumbed to apoptosis. Therefore, both the previous study and ours suggest that *MYC* overexpression in the alveolar epithelium induces hyperplasia that is eliminated by apoptosis.

In CTM mice and following resolution of hyperplasia in STM mice, MYC protein levels remained below the level of detection until the emergence of tumors (data not shown). Presumably stochastic events occurred that enabled tumorigenesis. Our data point to mutation of *Kras* as one of these stochastic events. We presume that *Kras* mutation is acquired spontaneously as the animal ages. It has long been known that MYC and activated RAS have the potential to cooperate in transformation (31). However, others have found *Kras* mutation in only a subset of *MYC*-induced murine lung tumors (30) or no mutations at all (32). This is in contrast to our finding that 100% of *MYC* transgenic tumors had an activating mutation in *Kras*. We cannot account for this discrepancy, other than to note that the composition of transgenes and the genetic backgrounds of the mice differed.

We sought to examine the tumor-initiating potential of *MYC*-induced hyperplastic cells. Our experiments using retrovirus that encodes mutant RAS to induce lung tumors in STM mice suggest that hyperplasias are, in fact, a cell population from which tumors can emerge. As pretreatment with DOX

Table 1. Demographic characteristics of human NSCLC cases used in survival analysis

		MYC IHC		
		Not expressed (%)	Expressed (%)	P[a]
n		41 (69.5)	18 (30.5)	
Age		66.9 ± 9.5	66.2 ± 7.9	0.77
Sex	Male	21 (51.2)	9 (50)	0.93
	Female	20 (48.8)	9 (50)	
Stage	I	31 (75.6)	14 (77.8)	0.33
	II	6 (14.6)	4 (22.2)	
	III	4 (9.8)	0 (0)	
Histology	ADC	32 (78.1)	7 (38.9)	0.0034
	SQCC	9 (21.9)	11 (61.1)	
Differentiation	WD	16 (39.0)	3 (16.7)	0.0394
	MD	14 (34.2)	4 (22.2)	
	PD	11 (26.8)	11 (61.1)	
MCL1 IHC	Low	25 (61.0)	5 (27.8)	0.0188
	High	16 (39.0)	13 (72.2)	

[a]Chi square analysis

Abbreviations: ADC, Adenocarcinoma; SQCC, Squamous cell carcinoma; WD, Well differentiated; MD, Moderately differentiated; PD, Poorly differentiated.

was required for the establishment of tumors, retroviral transduction presumably occurred in alveolar cells that responded to *MYC*-induction by proliferating. Thus, these experiments targeted mutant RAS expression directly to alveolar hyperplasia, supporting the view that cells with tumor-initiating potential reside within the hyperproliferative population.

Stem cells that are SPC$^+$, CCSP$^+$ and localized to the bronchioalveolar duct junction (BADJ) have been suggested to be the cell of origin for mouse adenomas and adenocarcinomas (33). However, in our mice, hyperplasia arose at the junctions of the alveolar septa, the anatomical location of type II cells. In addition, tumors from both CTM and STM mice expressed TTF-1 and SPC, proteins expressed in type II cells, but never Clara cell marker CCSP. If type II cells did give rise to alveolar hyperplasia and eventually to tumors, our experiments suggest that the right combination of oncogenic stimuli is able to initiate tumors from cells other than BADJ stem cells.

MYC-induced apoptosis impedes tumorigenesis

Our experiments suggest that a small enhancement of *MYC* activity can augment lung tumorigenesis. This phenomenon was easily discernable in STM mice given MNU or transduced with retrovirus expressing mutant RAS. In both cases, tumorigenesis was enhanced in mice kept free of DOX. This suggests that activated RAS promoted tumorigenesis in uninduced STM mice, where *MYC* was expressed above endogenous levels, but not above the threshold that induces apoptosis. When STM mice were treated with DOX, however, expression of *MYC* was induced to high levels and tumorigenesis diminished.

Previous work has defined distinctive thresholds for the various biological outputs of *MYC*. In particular, it has been shown that sustained expression of the gene at little more than physiological levels can elicit potentially tumorigenic proliferation of cells in diverse tissues (9). In contrast, higher levels of expression elicit tumor suppressor activities,

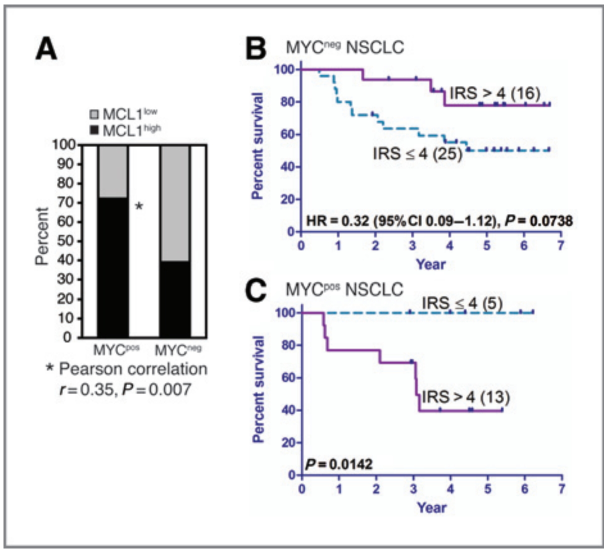

Figure 6. High MCL1 expression correlates with poor prognosis in human NSCLC coexpressing MYC. A, percentage of MYC-positive and MYC-negative human NSCLC that costained for high versus low levels of MCL1. MYC^{pos} tumors are those with an immunoreactive score (IRS) ≥ 1. MCL1^{high} tumors are those with an IRS > 4. B, Kaplan–Meier plot of MYC-negative NSCLCs dichotomized into MCL1^{high} (purple) and MCL1^{low} (blue) subsets. C, Kaplan–Meier plot of MYC positive NSCLCs dichotomized into MCL1^{high} (purple) and MCL1^{low} (blue) subsets. *P* values were estimated by Likelihood-ratio test.

including senescence and apoptosis. In the present instance, however, the *MYC* transgenic tumors and a subset of human NSCLCs both overexpressed MYC. This raises the question as to what additional genetic/epigenetic events have occurred over time that allow bypass of MYC-induced apoptosis.

MCL1 augments tumor progression when MYC is overexpressed

We utilized the tracheal delivery of retrovirus to STM mice to demonstrate that the combination of *Kras*^{G12V} and *Mcl1* was more potent than *Kras*^{G12V} alone in promoting tumor growth. However, the difference was only evident when the *MYC* transgene was activated by DOX treatment. Our data suggest that MCL1 overexpression is an acquired trait that can promote tumor progression by impeding MYC-induced apoptosis.

Consistent with this supposition, there was a positive correlation between high MCL1 and MYC expression in human NSCLC and the coexpression of these 2 factors correlated with poor patient survival. No prognostic significance could be attributed to MCL1 expression in the absence of MYC, which was consistent with previous observations (16, 17). We suggest that MCL1 overexpression mediates a shift in the threshold of MYC activity required to initiate apoptosis. This enables the selection of tumor cells expressing MYC and consequent tumor progression.

Implications for human malignancy

Our findings have several potential implications in regard to human malignancies. First, coexpression of MCL1 and MYC may serve as a useful biomarker for identifying aggressive forms of NSCLC and for predicting patient outcomes. Second, therapeutics directed at MCL1 may display a synthetic lethal interaction with MYC by exposing cells to MYC-induced apoptosis. Inhibitors of antiapoptotic BCL2-family proteins are now in clinical trials (34) and some are active against MCL1. Tumors that coexpress MYC and MCL1 might respond preferentially to inhibition of MCL1. Conversely, inhibiting antiapoptotic BCL2 family proteins other than MCL1 might fail in MYC-positive tumors when MCL1 levels are sufficient to protect against MYC-induced apoptosis. Third, to the best of our knowledge, this study is the first to demonstrate that MCL1 can partner with MYC in an epithelial malignancy, and this provides incentive to examine interactions between MCL1 and MYC in other such tumors.

Disclosure of Potential Conflicts of Interest

No potential conflicts of interest were disclosed.

Acknowledgments

We thank Luda Urisman for her help with the mouse colony and Dr. Dean Sheppard and Dr. Jeffrey Whitsett for supplying mice.

Grant Support

T.D. Allen, J.M. Bishop — G.W. Hooper Research Foundation
J.M. Bishop — N.I.H. Grant (CA009043),
M.S. Tsao — Canadian Cancer Society
N. Yanagawa — Terry Fox Foundation Training Program in Molecular Pathology of Cancer of the C.I.H.R. (STP-53912).

The costs of publication of this article were defrayed in part by the payment of page charges. This article must therefore be hereby marked *advertisement* in accordance with 18 U.S.C. Section 1734 solely to indicate this fact.

Received October 1, 2010; revised December 21, 2010; accepted January 12, 2011; published online March 15, 2011.

References

1. Meyer N, Penn LZ. Reflecting on 25 years with MYC. Nat Rev Cancer 2008;8:976–90.
2. Schlosser I, Holzel M, Hoffmann R, Burtscher H, Kohlhuber F, Schuhmacher M, et al. Dissection of transcriptional programmes in response to serum and c-Myc in a human B-cell line. Oncogene 2005;24:520–4.
3. Dang CV, O'Donnell KA, Zeller KI, Nguyen T, Osthus RC, Li F. The c-Myc target gene network. Semin Cancer Biol 2006;16:253–64.
4. van Riggelen J, Yetil A, Felsher DW. MYC as a regulator of ribosome biogenesis and protein synthesis. Nat Rev Cancer 2010;10:301–9.
5. Mitchell KO, Ricci MS, Miyashita T, Dicker DT, Jin Z, Reed JC, et al. Bax is a transcriptional target and mediator of c-myc-induced apoptosis. Cancer Res 2000;60:6318–25.
6. Soucie EL, Annis MG, Sedivy J, Filmus J, Leber B, Andrews DW, et al. Myc potentiates apoptosis by stimulating Bax activity at the mitochondria. Mol Cell Biol 2001;21:4725–36.
7. Juin P, Hueber AO, Littlewood T, Evan G. c-Myc-induced sensitization to apoptosis is mediated through cytochrome c release. Genes Dev 1999;13:1367–81.
8. Meyer N, Kim SS, Penn LZ. The Oscar-worthy role of Myc in apoptosis. Semin Cancer Biol 2006;16:275–87.
9. Murphy DJ, Junttila MR, Pouyet L, Karnezis A, Shchors K, Bui DA, et al. Distinct thresholds govern Myc's biological output in vivo. Cancer Cell 2008;14:447–57.
10. Yang T, Kozopas KM, Craig RW. The intracellular distribution and pattern of expression of Mcl-1 overlap with, but are not identical to, those of Bcl-2. J Cell Biol 1995;128:1173–84.
11. Clohessy JG, Zhuang J, de Boer J, Gil-Gomez G, Brady HJ. Mcl-1 interacts with truncated Bid and inhibits its induction of cytochrome c release and its role in receptor-mediated apoptosis. J Biol Chem 2006;281:5750–9.
12. Cuconati A, Mukherjee C, Perez D, White E. DNA damage response and MCL-1 destruction initiate apoptosis in adenovirus-infected cells. Genes Dev 2003;17:2922–32.
13. Beroukhim R, Mermel CH, Porter D, Wei G, Raychaudhuri S, Donovan J, et al. The landscape of somatic copy-number alteration across human cancers. Nature 2010;463:899–905.
14. Beverly LJ, Varmus HE. MYC-induced myeloid leukemogenesis is accelerated by all six members of the antiapoptotic BCL family. Oncogene 2009;28:1274–9.
15. Xiang Z, Luo H, Payton JE, Cain J, Ley TJ, Opferman JT, et al. Mcl1 haploinsufficiency protects mice from Myc-induced acute myeloid leukemia. J Clin Invest 2010;120:2109–18.
16. Borner MM, Brousset P, Pfanner-Meyer B, Bacchi M, Vonlanthen S, Hotz MA, et al. Expression of apoptosis regulatory proteins of the Bcl-2 family and p53 in primary resected non-small-cell lung cancer. Br J Cancer 1999;79:952–8.
17. Wesarg E, Hoffarth S, Wiewrodt R, Kroll M, Biesterfeld S, Huber C, et al. Targeting BCL-2 family proteins to overcome drug resistance in non-small cell lung cancer. Int J Cancer 2007;121:2387–94.
18. Perl AK, Tichelaar JW, Whitsett JA. Conditional gene expression in the respiratory epithelium of the mouse. Transgenic Res 2002;11:21–9.

19. Felsher DW, Bishop JM. Reversible tumorigenesis by MYC in hematopoietic lineages. Mol Cell 1999;4:199–207.
20. Nikitin AY, Alcaraz A, Anver MR, Bronson RT, Cardiff RD, Dixon D, et al. Classification of proliferative pulmonary lesions of the mouse: recommendations of the mouse models of human cancers consortium. Cancer Res 2004;64:2307–16.
21. Van Parijs L, Refaeli Y, Abbas AK, Baltimore D. Autoimmunity as a consequence of retrovirus-mediated expression of C-FLIP in lymphocytes. Immunity 1999;11:763–70.
22. Tsao MS, Aviel-Ronen S, Ding K, Lau D, Liu N, Sakurada A, et al. Prognostic and predictive importance of p53 and RAS for adjuvant chemotherapy in non small-cell lung cancer. J Clin Oncol 2007;25:5240–7.
23. Fisher GH, Wellen SL, Klimstra D, Lenczowski JM, Tichelaar JW, Lizak MJ, et al. Induction and apoptotic regression of lung adenocarcinomas by regulation of a K-Ras transgene in the presence and absence of tumor suppressor genes. Genes Dev 2001;15:3249–62.
24. Floyd HS, Farnsworth CL, Kock ND, Mizesko MC, Little JL, Dance ST, et al. Conditional expression of the mutant Ki-rasG12C allele results in formation of benign lung adenomas: development of a novel mouse lung tumor model. Carcinogenesis 2005;26:2196–206.
25. Johnson L, Mercer K, Greenbaum D, Bronson RT, Crowley D, Tuveson DA, et al. Somatic activation of the K-ras oncogene causes early onset lung cancer in mice. Nature 2001;410:1111–6.
26. Hydbring P, Bahram F, Su Y, Tronnersjo S, Hogstrand K, von der Lehr N, et al. Phosphorylation by Cdk2 is required for Myc to repress Ras-induced senescence in cotransformation. Proc Natl Acad Sci U S A 2010;107:58–63.
27. You M, Candrian U, Maronpot RR, Stoner GD, Anderson MW. Activation of the Ki-ras protooncogene in spontaneously occurring and chemically induced lung tumors of the strain A mouse. Proc Natl Acad Sci U S A 1989;86:3070–4.
28. Kozopas KM, Yang T, Buchan HL, Zhou P, Craig RW. MCL1, a gene expressed in programmed myeloid cell differentiation, has sequence similarity to BCL2. Proc Natl Acad Sci U S A 1993;90:3516–20.
29. Sun Z, Aubry MC, Deschamps C, Marks RS, Okuno SH, Williams BA, et al. Histologic grade is an independent prognostic factor for survival in non-small cell lung cancer: an analysis of 5018 hospital- and 712 population-based cases. J Thorac Cardiovasc Surg 2006;131:1014–20.
30. Rapp UR, Korn C, Ceteci F, Karreman C, Luetkenhaus K, Serafin V, et al. MYC is a metastasis gene for non-small-cell lung cancer. PLoS One 2009;4:e6029.
31. Land H, Parada LF, Weinberg RA. Tumorigenic conversion of primary embryo fibroblasts requires at least two cooperating oncogenes. Nature 1983;304:596–602.
32. Tran PT, Fan AC, Bendapudi PK, Koh S, Komatsubara K, Chen J, et al. Combined Inactivation of MYC and K-Ras oncogenes reverses tumorigenesis in lung adenocarcinomas and lymphomas. PLoS One 2008;3:e2125.
33. Kim CF, Jackson EL, Woolfenden AE, Lawrence S, Babar I, Vogel S, et al. Identification of bronchioalveolar stem cells in normal lung and lung cancer. Cell 2005;121:823–35.
34. Kang MH, Reynolds CP. Bcl-2 inhibitors: targeting mitochondrial apoptotic pathways in cancer therapy. Clin Cancer Res 2009;15:1126–32.